Plastic scintillator-based microfluidic devices for miniaturized detection of PET radiopharmaceuticals

Mark D. Tarn,[‡†][a][b] Mohammad M. N. Esfahani,[‡][a][c] Nuray Yavuzkanat Kızılyer,[‡§][d] Pankaj Joshi,[d] Nathaniel J. Brown,[c] Nicole Pamme,[b] David G. Jenkins,*[d] and Stephen J. Archibald*[a][b]

Abstract: A miniaturized radio-HPLC detector has been developed comprising a microfluidic device fabricated from plastic scintillator in combination with a silicon photomultiplier light sensor, and tested with samples containing a positron-emitting radionuclide [^{18}F]fluoride. This cost-effective, small footprint analytical tool is ideal for incorporation into integrated quality control systems for the testing of positron emission tomography (PET) radiopharmaceuticals to good manufacturing practice (GMP) standards.

Positron emission tomography (PET) is an important medical imaging technique for the diagnosis and monitoring of various conditions.[1] It relies upon the injection of a positron-emitting radiotracer into a patient, and subsequent detection of the radiolabelled drug within the body.[2] While conventional radiotracer production has followed a batch-based, centralised strategy, in which large batches of a single tracer are synthesised and distributed, there is currently a move towards decentralised and so-called "dose-on-demand" production.[3] In this case, single doses of a specific radiotracer would be generated on-site when required, enabling stratified patient treatment. However, this strategy necessitates the ability to manipulate small amounts of radioactivity and perform a number of processes in a rapid and automated fashion.

Microfluidic technology[4] presents an ideal means of meeting these requirements due to the small sizes and low volume fluid handling capabilities of these devices, and they have been successfully applied to the synthesis of PET radiotracers.[5] While this initial step has received a great deal of attention, subsequent stages have been largely neglected, particularly the stringent quality control (QC) tests required.[6] Several tests require the use of radiodetectors for radiochemical identity and purity determination, which are performed via the use of thin layer chromatography (radio-TLC) and high performance liquid chromatography (radio-HPLC). We are developing an integrated microfluidic QC platform for the testing of dose-on-demand PET radiotracers,[7] which, crucially, requires the inclusion of miniaturised radiodetectors for HPLC-style analysis.

Several examples of microfluidic or miniaturised radiodetectors have been demonstrated, with varying sensitivities, fabrication processes, and detection times that are summarised in a recent review by Ha et al.[6c] However, none of these are optimal for this application. Traditional autoradiography has been employed as a readily available method, but required exposure times on the order of hours to obtain an image of a microfluidic device; clearly unsuitable for real-time chromatography detection.[8] Cerenkov imaging enabled detection of radiation of a signal generated natively within the microfluidic device using only a charge-coupled device (CCD) camera, but acquisition times were around 5 min.[9] A PIN photodiode array was developed that allowed real-time detection of low levels of activity for pharmacokinetic studies, but had a complex microfabrication process that also required a thin microfluidic base to limit positron losses prior to their reaching the detector.[10] A miniaturised beta-particle camera system was also developed based on a position-sensitive avalanche photodiode (PSAPD) that enabled visualisation of activity within microfluidic devices, but again required complex fabrication steps and had an acquisition time of ≥1 min (although this does not necessarily indicate the limits of the detector).[11] Other novel radio-HPLC detection platforms of note have included a flow-through luminescence scintillation detector[12] and a parallel array of PET detector modules[13] that each demonstrated excellent performance but comprised relatively large pieces of apparatus.

In previous works we have demonstrated the direct detection of radiation via the use of miniaturised solid-state silicon photomultiplier light detectors (SiPMs) for half-life and activity measurements,[14] and the use of a hybrid silicon pixel detector for the imaging of radiation in a monolithic column.[15] Here, we demonstrate a new strategy offering complete integration of the device with the detector. This is based on the fabrication of microfluidic channels out of a plastic scintillator and their combination with SiPMs for the real-time detection of small volumes of a positron-emitting radioisotope, [^{18}F]fluoride, as part of a radio-HPLC system (Fig. 1a), towards its incorporation into an integrated QC platform.

[a] Dr. M. D. Tarn, Dr. M. M. N. Esfahani, Prof. S. J. Archibald
Positron Emission Tomography Research Centre, University of Hull, Cottingham Road, Hull, HU6 7RX (UK)
Email: s.j.archibald@hull.ac.uk
[b] Dr. M. D. Tarn, Prof. N. Pamme, Prof. S. J. Archibald
School of Mathematics and Physical Sciences, University of Hull, Cottingham Road, Hull, HU6 7RX (UK)
[c] Dr. M. M. N. Esfahani, Dr. N. J. Brown
School of Engineering and Computer Science, University of Hull, Cottingham Road, Hull, HU6 7RX (UK)
[d] Dr. N. Y, Kızılyer Dr. P. Joshi, Prof. D. G. Jenkins
Department of Physics, University of York, Heslington, York, YO10 5DD (UK)
Email: david.jenkins@york.ac.uk
[†] Current address: Dr. M. D. Tarn
School of Earth and Environment, University of Leeds, Woodhouse Lane, Leeds, LS2 9JT (UK)
[§] Current address: Dr. N. Y, Kızılyer
Faculty of Art and Science, Bitlis Eren University, Bitlis 13000 (Turkey)

‡ Authors contributed equally to this work.

Supporting information for this article is given via a link at the end of the document.

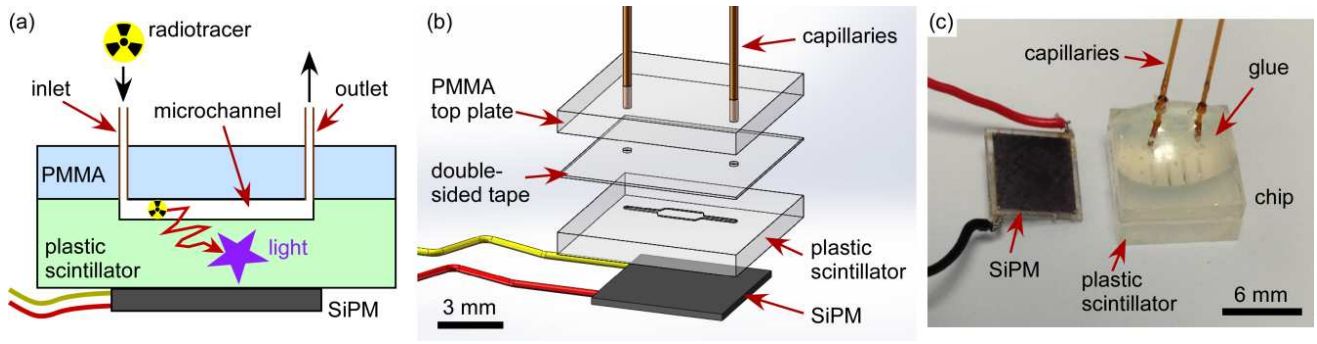

Figure 1. (a) Design principle of the microfluidic radio-HPLC detector fabricated from plastic scintillator. When a positron-emitting radioisotope (e.g. [^{18}F]fluoride) is injected into the device the positrons interact with the scintillator, generating light that is detected with a silicon photomultiplier (SiPM). (b) Exploded schematic of the microfluidic device consisting of a milled scintillator layer bonded to a PMMA top plate, with the SiPM placed below the chip. (c) Photograph of the assembled microfluidic device alongside an SiPM.

A scintillating material generates light upon interaction with radiation. Inorganic scintillators, e.g. thallium-doped sodium iodide (NaI(Tl)), are employed in conventional radio-HLPC together with a photomultiplier tube (PMT) for detection of the scintillation light. Plastic scintillators[16] typically consist of a base polymer, commonly polystyrene (PS) or polyvinyltoluene (PVT), that is doped with an organic "fluor" compound to provide the scintillation light, while some polymers are able to scintillate without doping.[16b] Inorganic[17] and plastic have previously been employed with microfluidic devices for the imaging of PET radiotracers, but required either integration times of at least 5 min[17a, 18] and/or camera-based detection,[17-18] were used to measure only high levels of activity,[3b] and required a thin baseplate of the microfluidic device in order to minimise positron losses. Furthermore, the combination of plastic scintillators with miniaturised SiPMs is already showing potential in a number of fields,[19] but has not yet been utilised for the radiodetection of PET radiopharmaceuticals. Furthermore, the ability to shape plastic scintillators using traditional polymer fabrication techniques, together with their high performance and low cost, makes them very attractive as a microfluidic substrate that combines fluid control with high signal detection efficiency.

The microfluidic radio-HPLC detector comprised a bottom layer fabricated from plastic scintillator (BC-404, Mi-Net Technology) into which a microchannel was milled, which was bonded to a non-scintillating PMMA top plate of 1 mm thickness (Fig. 1b,c). Three thicknesses of plastic scintillator were tested to evaluate the most effective of them: 1 mm, 2 mm and 3 mm thicknesses. The micochannel had a total internal volume of 0.7 µL. An SiPM (SensL, Ireland) was fixed beneath the plastic scintillator bottom layer and the assembly was wrapped in tape to block external light. The microfluidic chip was inserted into the flow path of a radio-HPLC system (1200 Series, Agilent, UK) via the capillary tubing. Plugs of a positron-emitting radioisotope, [^{18}F]fluoride, were injected into the HPLC with a mobile phase of water using an autosampler, with the injected activity first passing through a conventional NaI(Tl)/PMT radio-HPLC detector followed by the microfluidic radiodetector, allowing a direct comparison between the two.

Geant4 simulations were produced that showed the effect of plastic scintillator thickness on the measured dose (counts) in the presence of [^{18}F]fluoride (Fig. 2a). The results demonstrated that the maximum distance travelled by the emitted positrons should be in the range of 1.0 - 1.6 mm (with almost 90 % of positrons being stopped by 1.2 mm) in order to maximise the efficiency for positron interactions with the scintillator. This was tested experimentally by injecting 10 µL plugs of [^{18}F]fluoride (~150 MBq mL^{-1}) into microfluidic radiodetector chips having different thicknesses of the plastic scintillation layer (1 - 3 mm) (Fig. 3a), at a flow rate of 0.1 mL min^{-1}. The 2 mm and 3 mm thick scintillator chips yielded similar counts, as was expected since the counts should have been maximised within 1.6 mm as per the simulation. However, the 1 mm thick scintillator actually yielded a higher signal, despite the simulation indicating that the number of counts detected should not have reached the maximum for that thickness.

A study of the [^{18}F]fluoride energy spectra detected by the SiPM using 1 mm and 2 mm thick scintillator plates (Fig. 3b) yielded results that agreed with the simulation data shown in Figs. 2(a) and (b). The 2 mm thick scintillator was expected to allow full energy loss of the positrons emitted from [^{18}F]fluoride, while the higher energy positrons were expected to only be partially stopped in the 1 mm scintillator and, therefore, deposit less energy. The measured spectrum from the 2 mm scintillator clearly shows that the high energy tail of the positrons was shifted to lower energies. The total integrated area of the spectrum for all energies above above 250 keV (the peak of the positron emission for [^{18}F]fluoride) is approximately the same for both curves. This is expected as the activity of the [^{18}F]fluoride used was similar in both experiments. Below 250 keV it was not possible to compare the two spectra due to higher electronic thresholds that were used to keep the measurements free of electrical noise. The 1 mm thickness seemed to perform slightly better by having a better electrical signal-to-noise ratio and a lower end of the spectrum of 200 keV, while the 2 mm thick plate only showed a lower end of 250 keV. For this reason, 1 mm thick scintillator plates were chosen for further measurements. In future studies it would be beneficial to study the performance of even thinner scintillators. This should allow a better positron/gamma detection ratio and minimise errors from unwanted counting of gamma radiation. Thus, identifying the lowest scintillator thickness, without compromising the positron detection efficiency, would be very attractive.

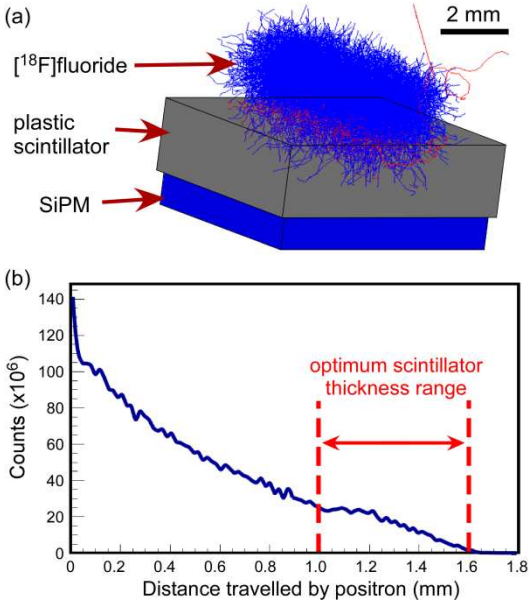

Figure 2. (a) Geant4 simulation of the positron emitting radioisotope, [^{18}F]fluoride, on a plastic scintillator with an SiPM underneath. The positrons (shown in blue) can be seen entering the scintillator plate. The red tracks indicate electrons and annihilation events caused by the interaction of positrons and electrons to generate anti-parallel 511 keV gamma rays. This simulation was run without gamma rays and their interactions. (b) Plot showing the number of positrons travelling through the plastic scintillator.

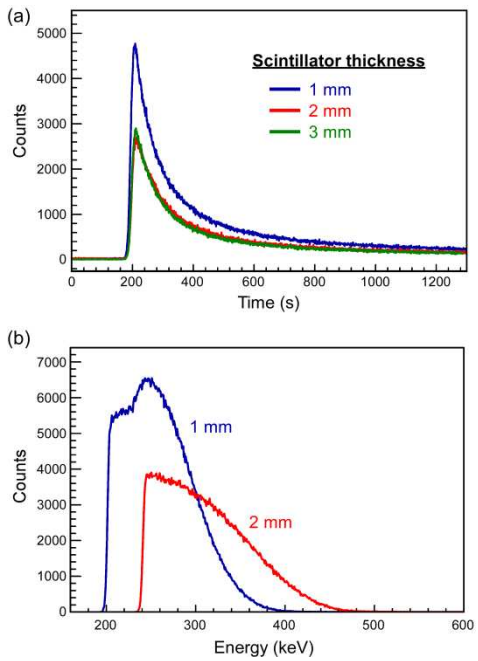

Figure 3. (a) Injections of 10 µL plugs of [^{18}F]fluoride (~150 MBq mL^{-1}) into microfluidic radio-HPLC detectors featuring plastic scintillation plates of differing thickness. (b) Pulse height energy spectrum of [^{18}F]fluoride generated in microfluidic chips with 1 mm and 2 mm thick scintillator plates. The energy spectrum was calibrated using two energy values: the highest energy of positrons (633 keV) and the mean energy of [^{18}F]fluoride (249.8 keV). The experimental setup and the threshold of the MCA were identical for each of the measurements.

To further test the response of the microfluidic radiodetector with a 1 mm thick plastic scintillator layer, 0.7 µL plugs of [^{18}F]fluoride (481 MBq mL^{-1}) were injected repeatedly into the HPLC flow path at a flow rate of 0.5 mL min^{-1}. The 0.7 µL injection volume was selected since this was the internal volume of the microchannel in the plastic scintillator layer of the microfluidic devices and so the detector device would be momentarily filled as the activity passed through. Fig. 4 shows the results for three injections of [^{18}F]fluoride (corrected for the time delay as the activity passed through the one detector and then the next), and demonstrates the ability to detect and resolve low volume plugs of injected activity in real-time using the microfluidic detector. The counts recorded by the microfluidic and conventional detector were found to be very similar, despite the fact that the former was part of a far smaller package in terms of both the scintillator and light detector, and with the detection zone also being far smaller. By comparison, the conventional detector consists of a coil of tubing through which the activity passes, situated below a 2" Ø x 8" tube containing the NaI(Tl) crystal and PMT.

The peaks shown in Figs. 3a and 4 are very broad, indicating retention of [^{18}F]fluoride in the system. This was an issue encountered in the HPLC instrument in general, rather than being specific to the microfluidic device and may be related to the multiple injection protocol used. We believe that some retention of [^{18}F]fluoride did occur in the chip and may have been caused by a number of factors that include the shape of the microchannel, the roughened scintillator surface caused by the micromilling process, and the use of double-sided tape to bond the top and bottom plates of the chip together. Improvements could be made in future iterations of the platform by using fabrication techniques such as hot embossing or polymer injection, together with solvent-based or thermal bonding. Passivation of the microfluidic channels could also be performed to prevent sample retention, while the use of different chip designs, such as a serpentine channel, may also be effective. Future tests will also involve the use of radiotracer samples rather than [^{18}F]fluoride which should reduce retention throughout the HLPC system.

Typical activities of radiotracer injected into a patient for a PET scan are ~370 MBq (10 mCi) in a volume that can typically vary from 0.5 - 15 mL, yielding a concentration range between 25 MBq mL^{-1} and 740 MBq mL^{-1}. Although the activities would likely be higher during QC testing even for dose-on-demand systems, since these tests must be completed before the dose is released, this provides a minimum activity level to consider. Therefore, the 150 MBq mL^{-1} activities detected in the 10 µL injected plugs (each thus containing ~1.50 MBq) and the 481 MBq mL^{-1} in the 0.7 µL plugs (i.e. 340 kBq) were each well within the appropriate range for QC testing. Furthermore, given the intensity of the peaks, it is expected that far lower activity levels would be detectable, and this would be explored during future optimisation and characterisation. Thus, the microfluidic radio-HPLC detectors were capable of detecting radiotracer levels relevant for QC testing of doses prior to clinical PET imaging.

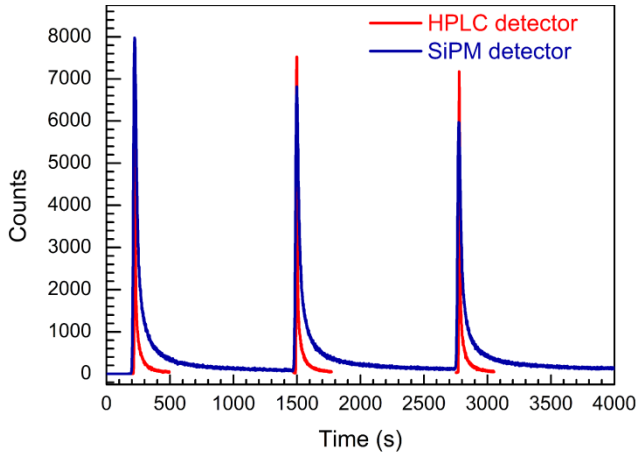

Figure 4. Multiple injections (0.7 µL) of plugs of [^{18}F]fluoride (481 MBq mL^{-1}) through a 1 mm thick plastic scintillator-based microfluidic radiodetector connected in series to a conventional NaI(Tl)/PMT radio-HPLC detector. Note that the conventional radio-HPLC automatically corrects for radioactive decay while the SiPM-based detector currently does not.

In summary, we have developed a miniaturised radio-HPLC detector for the QC analysis of PET radiotracers, based on a microfluidic device fabricated out of plastic scintillator and a small footprint, low-cost SiPM light sensor. The platform enabled real-time detection of [^{18}F]fluoride radioisotope with low injection volumes and clinically relevant levels of activity, while offering a far smaller and more versatile package compared to conventional NaI(Tl)/PMT radio-HPLC detectors to which it showed a similar response. This offers an inexpensive and customisable detection module that could be incorporated into an integrated QC platform for PET radiotracers produced via the dose-on-demand strategy. It should also be possible to produce the microfluidic devices using a number of plastic fabrication techniques, including embossing and injection moulding, that would extend the possibilities for channel customisation and make the device more amenable to mass fabrication. In particular, we envisage the incorporation of the detector into a monolith-based microfluidic HPLC separation for performing radiochemical identity and purity testing, with monolithic column-based HPLC platforms[20] have proven suitable for the testing of pharmaceuticals[21] and PET chemistry,[22] while monoliths have also already seen a number of applications in microfluidics for PET chemistry[15, 23] and other areas of radiochemistry.[24]

With further characterisation and optimisation of the design and configuration of the platform, we believe it should be possible to detect even lower volumes and levels of activity than those shown in these proof-of-concept tests. If significantly low limits of detection could be achieved, the platform may also have the potential for quantification of radiotracer metabolism in the blood of small animals during new tracer development.[10, 25]

Experimental Section

The microfluidic radio-HPLC detector was fabricated from two layers of plastic: a top layer consisting of a 1 mm thick non-scintillating PMMA plate, and a bottom layer fabricated from BC-404 plastic scintillator (Mi-Net Technology Ltd., UK) that was selected for its fast counting and suitability for beta particle (e.g. positron) detection.[26] A microchannel was milled[27] directly into the plastic scintillator layer to a depth of 50 µm, and three thicknesses of plastic scintillator were tested to evaluate the most effective of them: 1 mm, 2 mm and 3 mm thicknesses. The design comprised an inlet channel and an outlet channel (300 µm width) with a 1.7 mm x 1 mm chamber between them, yielding a total internal volume of 0.7 µL. The PMMA top plate featured only an inlet hole and an outlet hole, and it was bonded to the plastic scintillator bottom plate with double-sided tape into which access holes had been cut out. Fused silica capillary (150 µm i.d., 363 µm o.d.) was glued into the access holes for fluid transport.

An SiPM (C-Series, SensL, Ireland)[28] was positioned beneath the microfluidic chip, against the plastic scintillator. The entire assembly was wrapped in polytetrafluoroethylene (PTFE) tape to reflect generated scintillation light back to the SiPM, thereby maximising the amount of light detected, and then additionally wrapped in black electrical tape to hold the SiPM in place and to prevent external light reaching it. The SiPM was connected to a high voltage power supply and a preamplifier, with the preamplifier output then connected to a multi-channel analyser (MCA; MCA-527 Micro, GBS Electronik GmbH, Germany) for signal output (energy and activity spectra). Measurements were recorded from the MCA using WinSpec spectroscopy software (Princeton Instruments, USA) at a sampling rate of 1 reading per second.

Positron-emitting [^{18}F]fluoride radioisotope was generated via a compact low energy self-shielded cyclotron (BG75, ABT Molecular Imaging, USA)[3c, 3d] and diluted in water to the desired activity.

Acknowledgements

The authors from the University of Hull acknowledge the Daisy Appeal charity (grant no. DAhul2011) and HEIF (University of Hull) for funding, and thank Dr Assem Allam and his family for the generous donation to help found the PET Research Centre at the University of Hull and for their continued support. N. Y, K. acknowledges studentship support from the Turkish Government. The authors thank Gonçalo S. Clemente for preparation of [^{18}F]fluoride.

Keywords: plastic scintillator • silicon photomultiplier (SiPM) • microfluidics • radiopharmaceuticals • radio-HPLC

[1] M. E. Phelps, *Ann. Rev. Nucl. Part. Sci.* **2002**, *52*, 303-338.

[2] S. L. Pimlott, A. Sutherland, *Chem. Soc. Rev.* **2011**, *40*, 149-162.

[3] a) P. Y. Keng, M. Esterby, R. M. Van Dam, Emerging Technologies for Decentralized Production of PET Tracers, in *Positron Emission Tomography - Current Clinical and Research Aspects* (Ed.: C.-H. Hsieh), InTech, **2012**; b) V. Arima, G. Pascali, O. Lade, H. R. Kretschmer, I. Bernsdorf, V. Hammond, P. Watts, F. De Leonardis, M. D. Tarn, N. Pamme, B. Z. Cvetkovic, P. S. Dittrich, N. Vasovic, R. Duane, A. Jaksic, A. Zacheo, A. Zizzari, L. Marra, E. Perrone, P. A. Salvadori, R. Rinaldi, *Lab Chip* **2013**, *13*, 2328-2336; c) V. Awasthi, J. Watson, H. Gali, G. Matlock, A. McFarland, J. Bailey, A. Anzellotti, *Appl. Radiat. Isot.* **2014**, *89*, 167-175; d) A. Anzellotti, J. Bailey, D. Ferguson, A. McFarland, P. Bochev, G. Andreev, V. Awasthi, C. Brown-Proctor, *J. Radioanal. Nucl. Chem.* **2015**, *305*, 387-401.

[4] M. D. Tarn, N. Pamme, Microfluidics, in *Elsevier Reference Module in Chemistry, Molecular Sciences and Chemical Engineering* (Ed.: J. Reedijk), Elsevier, Waltham, MA, **2013**, doi: 10.1016/b978-0-12-409547-2.05351-8.

[5] a) G. Pascali, P. Watts, P. A. Salvadori, *Nucl. Med. Biol.* **2013**, *40*, 776-787; b) C. Rensch, A. Jackson, S. Lindner, R. Salvamoser, V. Samper, S. Riese, P. Bartenstein, C. Wängler, B. Wängler, *Molecules* **2013**, *18*, 7930-7956; c) P. Y. Keng, M. Sergeev, R. M. van Dam, Advantages of Radiochemistry in Microliter Volumes, in *Perspectives on Nuclear Medicine for Molecular Diagnosis and Integrated Therapy* (Eds.: Y. Kuge, T. Shiga, N. Tamaki), Springer Japan, Tokyo, **2016**, pp. 93-111.

[6] a) J. C. Hung, *J. Nucl. Med.* **2002**, *43*, 1495-1506; b) S. Yu, *Biomed. Imag. Interv. J.* **2006**, *2*, e57; c) N. Ha, S. Sadeghi, R. van Dam, *Micromachines* **2017**, *8*, 337; d) J. Ly, N. S. Ha, S. Cheung, R. M. van Dam, *Anal. Bioanal. Chem.* **2018**.

[7] a) M. D. Tarn, N. J. Brown, N. Pamme, S. J. Archibald, *J. Label. Compd. Radiopharm.* **2015**, *58*, S20; b) S. J. Archibald, N. Pamme, N. J. Brown, M. D. Tarn, *J. Nucl. Med.* **2015**, *56*, *suppl. 3*, 167; c) M. D. Tarn, A. Isu, S. J. Archibald, N. Pamme, in *The 18th International Conference on Miniaturized Systems for Chemistry and Life Sciences (MicroTAS 2014)*, San Antonio, TX, USA, **2014**, pp. 1077-1079; d) M. D. Tarn, M. M. N. Esfahani, Y. C. Chan, J. X. Buch, C. C. Onyije, P. J. Gawne, D. J. B. Gambin, N. J. Brown, S. J. Archibald, N. Pamme, in *The 21st International Conference on Miniaturized Systems for Chemistry and Life Sciences (MicroTAS 2017)*, Savannah, GA, USA, **2017**, pp. 559-560.

[8] M. Laven, I. Velikyan, M. Djodjic, J. Ljung, O. Berglund, K. Markides, B. Langstrom, S. Wallenborg, *Lab Chip* **2005**, *5*, 756-763.

[9] a) J. S. Cho, R. Taschereau, S. Olma, K. Liu, Y.-C. Chen, C. K. F. Shen, R. M. van Dam, A. F. Chatziioannou, *Phys. Med. Biol.* **2009**, *54*, 6757-6771; b) A. A. Dooraghi, P. Y. Keng, S. Chen, M. R. Javed, C.-J. C. J. Kim, A. F. Chatziioannou, R. M. van Dam, *Analyst* **2013**, *138*, 5654-5664.

[10] L. Convert, F. G. Baril, V. Boisselle, J.-F. Pratte, R. Fontaine, R. Lecomte, P. G. Charette, V. Aimez, *Lab Chip* **2012**, *12*, 4683-4692.

[11] C. Fang, Y. Wang, N. T. Vu, W.-Y. Lin, Y.-T. Hsieh, L. Rubbi, M. E. Phelps, M. Müschen, Y.-M. Kim, A. F. Chatziioannou, H.-R. Tseng, T. G. Graeber, *Cancer Res.* **2010**, *70*, 8299-8308.

[12] D. Thonon, G. Kaisin, J. Henrottin, J. Aerts, H. Van Malderen, A. Luxen, *Appl. Radiat. Isot.* **2013**, *73*, 84-89.

[13] J. S. Huber, S. M. Hanrahan, W. W. Moses, S. E. Derenzo, B. W. Reutter, J. P. O'Neill, G. T. Gullberg, in *2009 IEEE Nuclear Science Symposium Conference Record*, Orlando, FL, **2009**, pp. 2620-2624.

[14] M. P. Taggart, M. D. Tarn, M. M. N. Esfahani, D. M. Schofield, N. J. Brown, S. J. Archibald, T. Deakin, N. Pamme, L. F. Thompson, *Lab Chip* **2016**, *16*, 1605-1616.

[15] M. D. Tarn, D. Maneuski, R. Alexander, N. J. Brown, V. O'Shea, S. L. Pimlott, N. Pamme, S. J. Archibald, *Chem. Commun.* **2016**, *52*, 7221-7224.

[16] a) S. W. Moser, W. F. Harder, C. R. Hurlbut, M. R. Kusner, *Radiat. Phys. Chem.* **1993**, *41*, 31-36; b) G. H. V. Bertrand, M. Hamel, F. Sguerra, *Chem. Eur. J.* **2014**, *20*, 15660-15685; cL. Beaulieu, S. Beddar, *Phys. Med. Biol.* **2016**, *61*, R305.

[17] a) J. S. Cho, N. T. Vu, Z. T. F. Yu, R. W. Silverman, R. Taschereau, T. Hsian-Rong, A. F. Chatziioannou, in *2007 IEEE Nuclear Science Symposium Conference Record, Vol. 6*, Honolulu, HI, USA, **2007**, pp. 4615-4619; b) S. Türkcan, J. Nguyen, M. Vilalta, B. Shen, F. T. Chin, G. Pratx, P. Abbyad, *Anal. Chem.* **2015**, *87*, 6667-6673.

[18] J. S. Cho, N. T. Vu, Y. H. Chung, Z. T. Yu, R. W. Silverman, R. Taschereau, H. R. Tseng, A. F. Chatziioannou, in *IEEE 2006 Nuclear Science Symposium Conference Record, Vol. 4*, San Diego, CA, **2006**, pp. 1977-1981.

[19] a) M. P. Taggart, C. Payne, P. J. Sellin, *J. Phys. Conf. Ser.* **2016**, *763*, 012007; b) P. W. Cattaneo, M. D. Gerone, F. Gatti, M. Nishimura, W. Ootani, M. Rossella, Y. Uchiyama, *IEEE Trans. Nucl. Sci.* **2014**, *61*, 2657-2666; c) C. Liao, H. Yang, *Nucl. Instrum. Methods Phys. Res., Sect. A* **2015**, *789*, 150-157.

[20] a) F. Svec, Y. Lv, *Anal. Chem.* **2015**, *87*, 250-273; b) G. Guiochon, *J. Chromatogr. A* **2007**, *1168*, 101-168; c) I. Ali, V. D. Gaitonde, H. Y. Aboul-Enein, *J. Chromatogr. Sci.* **2009**, *47*, 432-442; d) H. Kobayashi, T. Ikegami, H. Kimura, T. Hara, D. Tokuda, N. Tanaka, *Anal. Sci.* **2006**, *22*, 491-501; e) O. Núñez, K. Nakanishi, N. Tanaka, *J. Chromatogr. A* **2008**, *1191*, 231-252.

[21] C. K. Zacharis, *J. Chromatogr. Sci.* **2009**, *47*, 443-451.

[22] D. J. Schenk, C. J. Welch, V. Antonucci, *J. Label. Compd. Radiopharm.* **2016**, *59*, 391-397.

[23] a) R. Ismail, J. Irribaren, M. R. Javed, A. Machness, R. Michael van Dam, P. Y. Keng, *RSC Adv.* **2014**, *4*, 25348-25356; b) P. He, B. P. Burke, G. S. Clemente, N. Brown, N. Pamme, S. J. Archibald, *React. Chem. Eng.* **2016**, *1*, 361-365.

[24] a) M. Losno, I. Ferrante, R. Brennetot, J. Varlet, C. Blanc, B. Grenut, E. Amblard, S. Descroix, C. Mariet, *Micromachines* **2016**, *7*, 45; b) M. Losno, I. Ferrante, R. Brennetot, S. Descroix, C. Mariet, *Procedia Chem.* **2016**, *21*, 446-452; c) A. Bruchet, V. Taniga, S. Descroix, L. Malaquin, F. Goutelard, C. Mariet, *Talanta* **2013**, *116*, 488-494.

[25] H. M. Wu, G. Sui, C. C. Lee, M. L. Prins, W. Ladno, H. D. Lin, A. S. Yu, M. E. Phelps, S. C. Huang, *J. Nucl. Med.* **2007**, *48*, 837-845.

[26] Data sheet for Premium Plastic Scintillators, Saint-Gobain, www.crystals.saint-gobain.com/sites/imdf.crystals.com/files/documents/sgc-bc400-404-408-412-416-data-sheet.pdf.

[27] D. J. Guckenberger, T. E. de Groot, A. M. D. Wan, D. J. Beebe, E. W. K. Young, *Lab Chip* **2015**, *15*, 2364-2378.

[28] a) SensL webpage, www.sensl.com, accessed August 2015; b) *Technical Note: Introduction to the SPM*, SensL, Ireland.